Minerals Engineering 36–38 (2012) 237–241

Contents lists available at SciVerse ScienceDirect

Minerals Engineering

journal homepage: www.elsevier.com/locate/mineng

On the origin of bi-modal bubble size distributions in the absence of frother ☆

J.J. Quinn, J.A. Finch *

Department of Mining and Materials Engineering, McGill University, 3610 University Street, Montreal, QC, Canada H3A 0C5

ARTICLE INFO

Article history:
Available online 9 May 2012

Keywords:
Bubble break-up
Coalescence-induced break-up
Coalescence
Bubble size
Liquid jet
Droplet

ABSTRACT

Several authors have noted bi-modal bubble size distributions (BSDs) in flotation systems at low frother or inorganic salt concentrations. The origin appears to be related to bubble–bubble interactions. The present work examines interactions among bubbles produced at a capillary using high-speed imaging. The study provides visual evidence of coalescence-related and wake-related mechanisms creating fine bubbles and bi-modal distributions. Four coalescence mechanisms are identified: coalescence-induced break-up, droplet formation and collision, liquid jet formation and collision, liquid jet disruption to droplets and collision; and two wake-related events: distortion and break-up of trailing bubble, and premature detachment. Comparing to the fine/coarse mode ratio in flotation systems (ca. 1/10) the possible relevant mechanisms are suggested. Knowing that frothers and certain inorganic salts act to retard coalescence, the origin of the bi-modal BSD is argued to be coalescence-related.

1. Introduction

Bubble formation in flotation machines results from an interplay of the gas dispersing device and solute properties. In the absence of coalescence-inhibiting agents bi-modal bubble size distributions (BSDs) are often observed (Quinn et al., 2007; Finch et al., 2008; Cappuccitti and Nesset, 2009; Yañez et al., 2009; Acuña and Finch, 2010).

Fig. 1 shows an example of a bi-modal BSD with supporting visual evidence observed in water in a laboratory flotation column with a porous sparger processing a Pb/Zn ore (Quinn et al., 2007). The water-only system produced a fine mode at ca. 0.5 mm and a coarse mode at ca. 5 mm (i.e., fine/coarse ratio ca. 1/10). The fine mode and the bi-modal distribution are eliminated in the presence of frother (10 ppm MIBC) replaced by a mono-modal distribution centered ca. 1.5 mm. Quinn et al. found >0.2 M NaCl likewise eliminated the bi-modal distribution.

In another example, Finch et al. (2008) show bi-modal distribution in a mechanical cell in water only with a fine mode (ca. 0.5 mm) and coarse mode (ca. 5 mm), i.e., ca. 1/10 ratio similar to Fig. 1. Sequential addition of frother was illustrated to progressively eliminate the bi-modal distribution eventually realizing a mono-modal distribution centered in that case at ca. 0.8 mm.

The origin of the bi-modal distribution in water only and its elimination by adding frother, or salt, needs an explanation. One possible origin of the bi-modal distribution is the fact that the large bubbles expected without frother are unstable and prone to break-up (Leighton et al., 1991). Another possibility is that the bi-modal distribution originates from bubble–bubble interactions. Tse et al. (2003), trying to explain the origin of fine bubbles as the swarm rose in a bubble column, observed coalescing bubbles expelling a fine bubble. They argued that an annular wave is set up in the newly formed bubble which travels the length of the bubble resulting in extension and pinching-off of a daughter bubble. The mechanism was observed in experiments contacting two bubbles at facing capillaries. The process will be called 'coalescence-induced bubble break-up'. Ohnishi et al. (1999) described a similar phenomenon.

Zhang and Thoroddsen (2008) studied coalescence-induced break-up. Experimentally, they launched one bubble into a second bubble held at a capillary and showed that for equal sized parent bubbles, the daughter bubble is roughly 1/10th the parent size. Using high-speed video imaging the authors identified the capillary waves which converged at the bubble apex and pinched off the daughter bubble.

Exploring the origin of bi-modal distributions in the absence of frother in flotation systems, Finch et al. (2008) found they could control bubble interactions and generate coalescence-induced break-up by manipulating gas rate at a capillary. In the example shown, addition of frother prevented coalescence and the related fine bubble formation. The intention was to pursue this experimental technique and determine the gas rate at which coalescence-induced break-up occurred as a function of frother addition, following similar previous work that tracked the transition gas rate between non-coalescence and coalescence (Kracht and Finch, 2009). It became apparent, however, that the mechanism described by Tse et al. was only one possibility. The purpose of this paper is to identify other mechanisms that may promote

☆ Paper is based on the keynote lecture by J.A. Finch.

* Corresponding author.
E-mail addresses: jarrett.quinn@mail.mcgill.ca (J.J. Quinn), jim.finch@mcgill.ca (J.A. Finch).

0892-6875/$ - see front matter © 2012 Elsevier Ltd. All rights reserved.
http://dx.doi.org/10.1016/j.mineng.2012.04.001

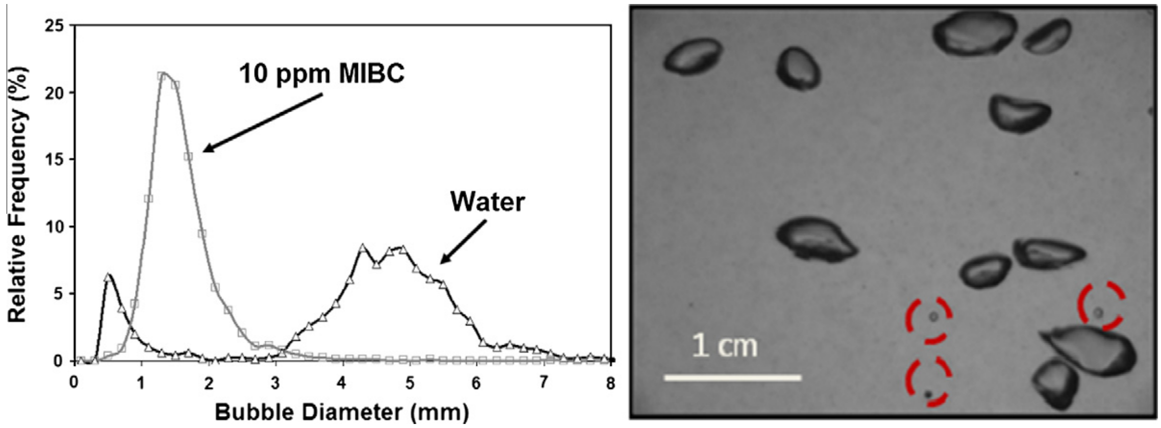

Fig. 1. Left: Bubble size distribution (number frequency) in water and 10 ppm MIBC solution. Right: Example image showing large irregular shaped bubbles and fine bubbles (identified by dashed circle) in the water-only system. (Reprinted (modified) from Minerals Engineering, Quinn, J.J., Kracht, W., Gomez, C.O., Gagnon, C., and Finch, J.A., Comparing the effect of salts and frother (MIBC) on gas dispersion and froth properties. 20, 1296–1302, 2007, with permission from Elsevier.)

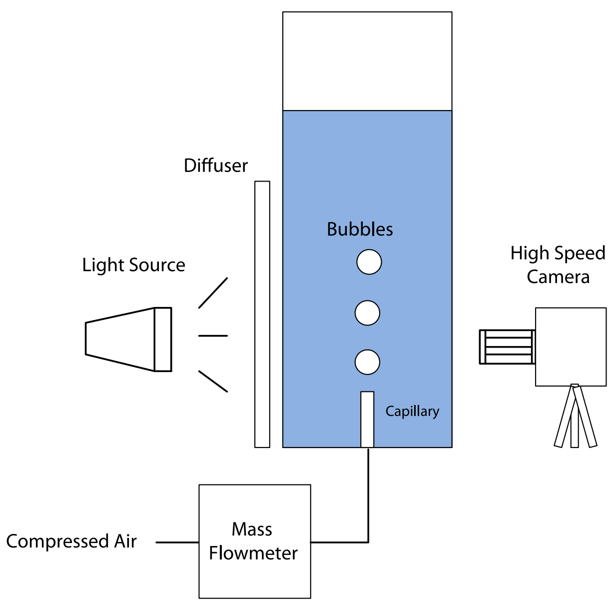

Fig. 2. Experimental set-up.

small bubble formation and bi-modal distributions using high speed imaging of bubble interactions at a capillary.

2. Experimental

The experimental set-up (Fig. 2) comprised a 50 cm (l) × 20 cm (w) × 50 cm (h) acrylic tank holding 30 L Montreal tap water (average conductivity: 293 μS/cm, major constituents: 30 mg/L Ca, 24 mg/L SO_4, 23 mg/L Cl, 13 mg/L Na, 8 mg/L Mg (Remillard et al., 2009)) in which air bubbles were formed at a glass capillary tube with internal diameter of nominally 500 μm (508 ± 25.4 μm). The water was at room temperature, 20–22 °C. Air flow rate was regulated using a Sierra model 840DL1V1 (0–500 sccm) mass flow meter controller. Tests were operated at air flow rates ranging from 70 to 250 sccm.

A Fastec Toubleshooter HR digital high-speed camera equipped with a 60 mm macro lens (Nikon, AFMicro Nikkor) was used to capture events close to the point of generation. Images (320 × 240 px) were collected at rates of 500–2000 frames per second.

Bubble size estimates were made for the coarse and fine bubbles shown in the example images. Large bubbles assumed an oblate ellipsoidal shape typically 10–20 mm above the point of generation. Images taken under these conditions were analyzed using ImageJ software. An ellipse was fitted to the bubble with major (a) and minor (b) semi-axis being calculated. An equivalent diameter (d_e) was calculated based on the following equation:

$$d_e = \sqrt[3]{(2a)^2 \times (2b)} \tag{1}$$

Due to the fine bubble sizes obtained and the image resolution, fine bubble sizes were estimated by manual inspection using ImageJ software.

3. Results

Six mechanisms resulting in fine bubbles were observed, four related to coalescence and two to wake effects.

3.1. Coalescence-induced

3.1.1. Bubble break-up

Fig. 3 shows a sequence of events at the 500 μm capillary with air flow rate 70 sccm. The sequence shows coalescence (at 1.0 ms) and subsequent bubble detachment from the orifice (3.0 ms) to produce the capillary wave which travels up the bubble and leads to the expulsion of a fine bubble (12.5–13.0 ms). The equivalent spherical diameter of the large bubble is ca. 3.6 mm (equivalent spherical diameter), and the fine bubble is ca. 0.4 mm, i.e., ca. 1/9th the parent bubble size.

3.1.2. Droplet formation, collision and bubble expulsion

The image sequence in Fig. 4 was taken under the same conditions as those in Fig. 3. In this case, however, there is evidence of coalescence-induced droplet formation inside the newly created bubble. The droplet is formed as the trailing edge of the bubble recoils soon after detachment from the orifice (6–8 ms). The droplet travels the length of the bubble (6–12 ms) and impacts the forward bubble wall (14 ms) which in this example expels two small daughter bubbles (16 ms). The parent bubble is ca. 4.0 mm while the daughter bubbles are ca. 0.4 and 0.2 mm (ca. 1/10th and 1/20th the parent bubble size).

3.1.3. Jet formation, collision and bubble expulsion

Increasing air flow rate to 250 sccm, instead of the droplet, the liquid enters the bubble as a jet (Fig. 5, at 3 ms) which shoots through the opposite bubble wall, this time expelling three fine